# Chain Conformation of a New Class of PEG-Based Thermoresponsive Polymer Brushes Grafted on Silicon as Determined by Neutron Reflectometry

Xiang Gao,[†] Norbert Kučerka,[‡] Mu-Ping Nieh,[‡] John Katsaras,[‡] Shiping Zhu,*,[†] John L. Brash,[†] and Heather Sheardown[†]

[†]*Department of Chemical Engineering, McMaster University, Hamilton, Ontario, Canada, L8S 4L7, and* [‡]*Canadian Neutron Beam Centre, National Research Council, Chalk River, Ontario, Canada, K0J 1J0*

The thermoresponsive PEG-based copolymer poly[2-(2-methoxyethoxy)ethyl methacrylate-*co*-oligo(ethylene glycol) methacrylate) (P(MEO$_2$MA-*co*-OEGMA)] was grafted onto a silicon wafer, and its chain conformation in aqueous solution was studied by neutron reflectometry. The effects of temperature and salt concentration on the polymer's conformation were evaluated. With increasing temperature, it was found that the polymer brushes underwent a transition from an extended state to a compressed state, and eventually a collapsed state above the lower critical solution temperature. The presence of salt significantly affected the well-extended brushes but had little effect on compressed and collapsed brushes. This PEG-based thermoresponsive surface exhibited good protein adsorption resistance. Interestingly, extended and collapsed brushes showed the same level of protein repulsion, something that was not expected.

## Introduction

In past decades, surface modification techniques have played important roles in biology and medicine fields for various purposes (e.g., antifouling of surfaces by proteins). Recently, there have been many novel areas developed that require so-called "smart biological surfaces", which can respond to external stimuli such as solvent type, pH, temperature, electric and magnetic fields, and so forth.[1−6] These smart surfaces can alter their properties (e.g., hydrophilicity, biological activity, protein adsorption/repulsion, cell adhesion, migration, and so forth) in response to small changes in the external environment. In fact, there are potentially significant applications in the areas of bioseparation, diagnostics, drug delivery, gene therapy, and implants. Furthermore, these surfaces are able to recognize biological events by emitting measurable electronic or optoelectronic signals. As such, they can be used as biosensors for bioanalysis, clinical diagnosis, and environmental monitoring.

Among smart surfaces, thermoresponsive surfaces, which can respond to temperature variations, are some of the most important (since temperature, as a stimulus, can be easily regulated). Moderate changes in temperature close to physiological temperature have practically little effect on the biosystem. As a result, many thermoresponsive surfaces have been developed. Until recently, thermoresponsive materials have mainly been limited to poly(*N*-isopropylacrylamide) (PNIPAM) and its copolymers.[7−9] PNIPAM has a lower critical solution temperature (LCST) of 32 °C, between room temperature and physiological temperature. Below its LCST, the surface polymer brushes in solution are in the well-extended conformation. However, when the temperature is above 32 °C, the polymer chains undergo a sharp phase transition, forming a collapsed layer. A sharp change in surface properties is thus trigged by a moderate temperature stimulus. As a result of this property, thermoresponsive surfaces based on PNIPAM have been developed for various applications.

Recently, a new class of biocompatible thermoresponsive material, namely, poly[2-(2-methoxyethoxy)ethyl methacrylate-*co*-oligo(ethylene glycol) methacrylate) (P(MEO$_2$MA-*co*-OEGMA)], has attracted much attention.[10−15] Similar to the amide group in PNIPAM, the oligo(ethylene glycol) in this copolymer has various hydrogen-bonding interactions with water when temperature varies, giving its thermoresponsive ability. This random copolymer has been shown to have a LCST in water. The phase transition is reversible and is almost independent of external conditions. Furthermore, the copolymer's LCST can be readily altered (from 26 to 92 °C), simply by varying the copolymer's composition. The great interest in these new thermoresponsive materials lies in the fact that they are entirely constructed with poly(ethylene glycol) methacrylate. Poly(ethylene glycol) (PEG)-based polymers are the most popular materials in biorelated applications because of their excellent resistance to nonspecific protein adsorption and cell adhesion, as well as their nontoxic and nonimmunogenic properties.

This new class of thermoresponsive polymer surfaces may lead to products that will hopefully be incorporated into various

*Corresponding author. zhuship@mcmaster.ca.

(1) Galaev, I. Y.; Mattiasson, B. *Trends Biotechnol.* **1999**, *17*(8), 335–340.
(2) Mendes, P. M. *Chem. Soc. Rev.* **2008**, *37*(11), 2512–2529.
(3) Sanjuan, S.; Tran, Y. *Macromolecules* **2008**, *41*(22), 8721–8728.
(4) Sanjuan, S.; Tran, Y. *J. Polym. Sci.: Polym. Chem.* **2008**, *46*(13), 4305–4319.
(5) Biesalski, M.; Johannsmann, D.; Ruhe, J. *J. Chem. Phys.* **2004**, *120*(18), 8807–8814.
(6) Biesalski, M.; Ruhe, J. *Macromolecules* **2002**, *35*(2), 499–507.
(7) Zhou, F.; Huck, W. T. S. *Phys. Chem. Chem. Phys.* **2006**, *8*(33), 3815–3823.
(8) Luzinov, I.; Minko, S.; Tsukruk, V. V. *Prog. Polym. Sci.* **2004**, *29*(7), 635–698.
(9) Liu, Y.; Mu, L.; Liu, B. H.; Kong, J. L. *Chem.-Eur. J.* **2005**, *11*(9), 2622–2631.

(10) Han, S.; Hagiwara, M.; Ishizone, T. *Macromolecules* **2003**, *36*(22), 8312–8319.
(11) Lutz, J. F.; Akdemir, O.; Hoth, A. *J. Am. Chem. Soc.* **2006**, *128*(40), 13046–13047.
(12) Lutz, J. F.; Hoth, A. *Macromolecules* **2006**, *39*(2), 893–896.
(13) Lutz, J. F.; Andrieu, J.; Uzgun, S.; Rudolph, C.; Agarwal, S. *Macromolecules* **2007**, *40*(24), 8540–8543.
(14) Yamamoto, S.; Pietrasik, J.; Matyjaszewski, K. *Macromolecules* **2007**, *40*(26), 9348–9353.
(15) Lutz, J. F. *J. Polym. Sci.: Polym. Chem.* **2008**, *46*(11), 3459–3470.

biomedical devices. So far, there have only been a few reports in the literature regarding this new thermoresponsive surface. In 2007, Huck et al.[16] grafted this copolymer onto a surface using the surface-initiated atom transfer radical polymerization (ATRP) method. The thermoresponsive collapse transition of polymer brushes on the surface was demonstrated by water contact angle measurements and liquid atomic force microscopy (AFM). In 2008, Lutz et al.[17] used the same type of thermoresponsive surface to control cell adhesion over the temperature range 25−37 °C. Glinel et al.[18] replaced OEGMA with a hydroxyl-terminated oligo(ethylene glycol) methacrylate (HOEGMA) monomer. A natural antibacterial peptide, magainin I, was then immobilized through grafting of hydroxyl group, giving an antibacterial surface. The amount of hydroxyl reactive groups could be readily adjusted by changing the monomer mixture composition.

Knowledge regarding the conformation of polymer brushes on a surface is crucial when designing smart surfaces. However, obtaining such information can be challenging, and as such, not much is known with regard to these new materials on the surface. Huck et al.[16] used the aqueous AFM method to study variations of polymer brush thickness in water as a function of temperature. As expected, brush thickness decreased when the temperature was raised above the copolymer's LCST. This work demonstrated a novel approach in the design of PEG-based thermoresponsive surfaces for biological and medical applications. However, it should be noted that in aqueous solutions AFM measurements are approximate. As polymer brushes in a good solvent are well-extended with dissolution into the solvent, the penetration of an AFM tip into polymer brushes can further complicate matters. The measured thicknesses strongly depend on the applied force (i.e., the stronger the applied force, the deeper the AFM tip penetrates into the brushes). Moreover, besides brush thickness there is other useful information (e.g., global brush conformation, water fraction surrounding the chains) needed in order to effectively design thermoresponsive devices.

Neutron and X-ray reflectometry have emerged as powerful, noninvasive surface/interface probes used to characterize the structures of materials on solid and liquid surfaces.[19−22] Here, we employed neutron reflectometry (NR) to study the conformation of polymer brushes on surfaces *in situ* in water. Importantly, thermal neutrons, because of their low energies (~10 meV), do not have any deleterious effect on sometimes fragile polymeric samples. Neutron reflectometry is also a bulk probe giving rise to the average polymer brush conformation over the entire sample. The water fraction inside the polymer brushes can also be estimated. Small changes in conformation in different environments can be monitored by the NR method.

Another issue that needs to be addressed with regard to these new thermoresponsive surfaces is their biocompatibility. A major advantage of this new class of PEG-based materials lies in their protein repulsion ability. However, there are still two concerns: First, about 90% of POEGMA have only two ethylene oxide

(EO) repeat units per side chain. Although homoPOEGMA has well been accepted as a biocompatible material, popular candidates often have 4.5 to 9 repeat EO units.[23−25] These new thermoresponsive copolymers with 90% POEGMA having only two EO repeat units have a more hydrophobic methacrylate backbone that may play an important role in determining the performance of the polymer. To the best of our knowledge, there are no reports on protein repulsion with regard to surfaces modified by this new type of PEG-based brush. Second, polymer brushes might lose their protein repelling ability in a collapsed state above LCST. Thermoresponsive surfaces have been used to control cell adhesion.[17,26] For example, Rimmer et al.[26] employed PNIPAM surfaces as culture for cells above LCST and found that the cells adhered on the collapsed PNIPAM chains. When the temperature was decreased below LCST, the extended PNIPAM chains expelled the cells. If these PEG-based thermoresponsive surfaces adsorb large amount of proteins when in the collapsed state, their potential applications could be limited. It is also fundamentally important to investigate and understand the relationship between polymer extension and their protein repelling ability.

The objective of this work is twofold. The first objective is to elucidate the detailed conformations of this new class of polymer brushes on substrates immersed in an aqueous environment, below and above the polymer's LCST, and to study the effects of some the influencing factors on their conformation. The second is to evaluate their resistance to protein adsorption. In particular, we want to compare their protein repelling performances below and above LCST.

## Experimental Section

**Materials.** $Cu^{I}Cl$ (99%), $Cu^{II}Cl_2$ (97%) and 2,2′-bipyridyl (Bipy) (99%) were purchased from Aldrich and used as received. 2-(2-Methoxyethoxy)ethyl methacrylate ($MEO_2MA$) (95%, $M_n = 188.22$ g/mol, Aldrich) and oligo(ethylene glycol) methacrylate (OEGMA) (98%, $M_n = 475$ g/mol, Aldrich) were distilled over $CaH_2$ under vacuum. Toluene (HPLC grade, Aldrich) was stirred over $CaH_2$ overnight and then distilled twice. Methanol (HPLC grade, Aldrich) was distilled over $CaH_2$ prior to use. Deionized water from the Millipore water purification system had the minimum resistivity of 18.0 MΩ·cm. Argon and nitrogen gases were of ultrahigh-purity grade. Silicon wafers (6 mm thick, 101.6 mm diameter) for neutron reflectometry experiments were purchased from Wafer World Inc. (West Palm Beach, FL). Silicon wafers for radiolabeled protein adsorption experiments had a thickness of 0.56 mm and were cut into $12 \times 6$ mm² pieces. Lysozyme was purchased from Sigma chemical Co. (St. Louis, MO) and used as received. The molecular weight and dimensions of lysozyme are 14 300 g/mol and $45 \times 30 \times 30$ Å³, respectively. All other materials were commercially available and used as received.

**Self-Assembly of Initiator Monolayer on Silicon Wafers.** The surface-attachable ATRP initiator, 6-(2-bromo-2-methyl) propionyloxy hexenyl trichlorosilane, was synthesized by the hydrosilylation of trichlorosilane with hex-6-en-1-yl 2-bromo-2-methylpropionate. Silicon wafers were pretreated as described previously.[27] They were then immersed in a 2.5 mM solution of 6-(2-bromo-2-methyl) propionyloxy hexenyl trichlorosilane in dry toluene for 18 h, at room temperature to form a self-assembled

(16) Jonas, A. M.; Glinel, K.; Oren, R.; Nysten, B.; Huck, W. T. S. *Macromolecules* **2007**, *40*(13), 4403–4405.

(17) Wischerhoff, E.; Uhlig, K.; Lankenau, A.; Borner, H. G.; Laschewsky, A.; Duschl, C.; Lutz, J. F. *Angew. Chem., Int. Ed.* **2008**, *47*(30), 5666–5668.

(18) Glinel, K.; Jonas, A. M.; Jouenne, T.; Leprince, J.; Galas, L.; Huck, W. T. S. *Bioconjugate Chem.* **2009**, *20*(1), 71–77.

(19) Kucerka, N.; Nieh, M. P.; Pencer, J.; Harroun, T.; Katsaras, J. *Curr. Opin. Colloid Interface Sci.* **2007**, *12*(1), 17–22.

(20) Yim, H.; Kent, M. S.; Huber, D. L.; Satija, S.; Majewski, J.; Smith, G. S. *Macromolecules* **2003**, *36*(14), 5244–5251.

(21) Yim, H.; Kent, M. S.; Mendez, S.; Lopez, G. P.; Satija, S.; Seo, Y. *Macromolecules* **2006**, *39*(9), 3420–3426.

(22) Zhang, J. M.; Nylander, T.; Campbell, R. A.; Rennie, A. R.; Zauscher, S.; Linse, P. *Soft Matter* **2008**, *4*(3), 500–509.

(23) Dormidontova, E. E. *Macromolecules* **2002**, *35*(3), 987–1001.

(24) Lee, B. S.; Lee, J. K.; Kim, W. J.; Jung, Y. H.; Sim, S. J.; Lee, J.; Choi, I. S. *Biomacromolecules* **2007**, *8*(2), 744–749.

(25) Ma, H. W.; Li, D. J.; Sheng, X.; Zhao, B.; Chilkoti, A. *Langmuir* **2006**, *22*(8), 3751–3756.

(26) Collett, J.; Crawford, A.; Hatton, P. V.; Geoghegan, M.; Rimmer, S. *J. R. Soc. Interface* **2007**, *4*(12), 117–126.

(27) Gao, X.; Feng, W.; Zhu, S. P.; Sheardown, H.; Brash, J. L. *Langmuir* **2008**, *24*(15), 8303–8308.

initiator monolayer with a thickness of $1.9 \pm 0.2$ nm. The silicon wafers were then removed from solution, ultrasonically cleaned in dry toluene, rinsed sequentially with toluene and methanol, and then dried in an argon stream.

**Grow P(MEO$_2$MA-*co*-OEGMA) Copolymer Brushes from Surface.** In a typical procedure of grafting P(MEO$_2$MA-*co*-OEGMA) copolymer brushes, Cu$^I$Cl (297 mg, 3.3 mmol), Cu$^{II}$Cl$_2$ (44.37 mg, 0.33 mmol), and Bipy (1632 mg, 10.41 mmol) were added into a 250 mL flask. The flask was then evacuated and backfilled with argon (procedure repeated 3 times). Degassed MEO$_2$MA (35.76 g, 190 mmol), OEGMA (4.75 g, 10 mmol), deionized water (66.7 mL), and methanol (33.3 mL) were then transferred into the flask. After degassing with argon for another hour, the mixture was transferred into a glovebox filled with ultrapure nitrogen, distributed into glass containers with the initiator-modified silicon wafers inside. The grafting process was carried out at room temperature for 200 min and stopped by adding a methanol solution of Cu$^{II}$Cl$_2$/Bipy, as shown in Scheme 1. The polymer-grafted silicon wafers were then ultrasonically cleaned in methanol, rinsed thoroughly, and dried in an argon stream. The comonomer ratio of MEO$_2$MA/OEGMA in the methanol/water solution was varied to achieve samples with different LCSTs. In this work, two ratios, MEO$_2$MA/OEGMA=95:5 (sample 1) and MEO$_2$MA/OEGMA = 85:15 (sample 2), were chosen.

**Characterization.** The thickness of grafted polymer layers on silicon wafers was measured by ellipsometry (Exacta 2000, Waterloo Digital Electronics) using a He−Ne laser (632.8 nm). The incident angle was set to 70°. The refractive index (*n*) and extinction coefficient (*k*) of Si ($n = 3.865$, $k = 0.020$) and SiO$_2$ ($n = 1.465$, $k = 0$) were used to determine the SiO$_2$ layer thickness. Values of $n = 1.500$ and $k = 0$ were used for the initiator and polymer layers. All the measurements were conducted in air at room temperature. A contact angle goniometer (model 200, Rame-Hart instrument Co.) was used to measure the water contact angle of the various surfaces. The advancing water contact angle was measured by the sessile drop method.

**Neutron Reflectometry Experiments.** NR experiments were carried out at the D3 reflectometer located at the National Research Universal (NRU) reactor (Chalk River, ON). 2.37 Å wavelength ($\lambda$) neutrons were chosen using a pyrolytic graphite monochromator. During the NR measurements, the neutron incident angle ($\theta$) and reflected angle ($2\theta$) were varied systematically, giving rise to the specular neutron momentum transfer $Q_z$: $Q_z = (4\pi \sin \theta)/\lambda$. The reflected intensity was recorded while the neutron momentum transfer $Q_z$ varied from 0.006 to 0.1 Å$^{-1}$. The data were normalized with respect to the incident beam intensity in order to account for any variation due to changes in slit width. The background was determined by offsetting the detector by $+ 0.5°$ (i.e., $2\theta + 0.5°$).

The samples were measured both in air and in aqueous solution. For the dry condition, the silicon wafer was placed on the sample table exposed to air. In this case, the path of the incident neutron beam was air → sample → SiO$_2$ → Si. In the case of samples in water (D$_2$O or D$_2$O buffer solutions), the silicon wafer was placed in a specially designed sample cell, described elsewhere.[28] The incident neutron beam path was Si → SiO$_2$ → sample → aqueous solution. The different path arrangements for dry and wet conditions were to ensure the total reflection condition at low angles.

PARRATT 32 (BENSC, Berlin) software was employed to analyze the data. In the case of dry samples, a three-layer (SiO$_2$, initiator monolayer, polymer layer) model was used. For samples in water, a stretched parabolic decay was added to the polymer

**Scheme 1. Synthesis Procedure for P(MEO$_2$MA-*co*-OEGMA) Copolymer Brushes on Silicon Wafer Surface via Surface-Initiated ATRP**
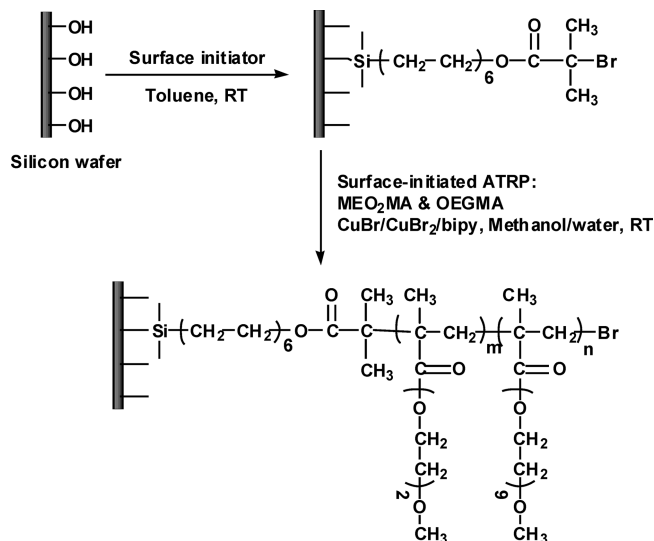


layer, as a result of the polymer chains extending into the aqueous environment. The stretched parabolic function used was as follows:[29] $\Phi_{poly}(z) = \Phi_{0,poly}[1 - (z/h)^2]^\alpha$, where $z$ is the distance from the interface, $\Phi_{poly}(z)$ is the polymer volume fraction at a distance $z$, and $\Phi_{0,poly}$ is the polymer volume fraction at a distance 0. The parameters $h$ and $\alpha$ modify the parabolic decay shape.

The best fit scattering length density (SLD, a function describing the density and atomic composition) profile normal to the surface was obtained by minimizing the chi squares ($\chi^2$). SLD profiles were then converted to volume fraction profiles based on the SLDs of the initiator layer, polymer layer, and D$_2$O. The SLD of the components was estimated from[30] SLD = $dN_A \Sigma b_i/M$, where $d$ is the mass density of the component, $N_A$ is Avogadro's number, $M$ is the molecular weight of the component, and $\Sigma b_i$ is the sum of the neutron scattering lengths of the various atoms making up the sample.

**Protein Adsorption Experiments.** Protein adsorption experiments were carried out in isotonic tris buffered saline (TBS) with radioiodinated proteins. In this work, lysozyme was chosen as the model protein. It is a small spherical protein with the dimension of $45 \times 30 \times 30$ Å$^3$, suitable for model studies. Its adsorption behavior on polymer surfaces has been studied in our previous work.[31] The iodine monochloride (ICl) method was employed to radiolabel lysozyme with Na125I (MP Biomedicals, Inc., Irvine, CA).[32] Unbound radioactive iodide was removed by ion exchange chromatography. The solutions for protein adsorption contained 10% radiolabeled lysozyme. The surfaces were first kept in TBS solution for 12 h in order to completely hydrate the polymer brushes. Surfaces were then immersed in the protein solution for 2 h allowing protein adsorption to reach equilibrium. The samples were then put into fresh TBS solution for 5 min (3 cycles) to remove any loosely adsorbed protein. The samples were then dried and measured by a Wizard 3″ 1480 Automatic Gamma Counter (Perkin-Elmer Life Sciences) to determine the amount of proteins adsorbed onto each surface.

## Results and Discussion

**Ellipsometry and Contact Angle Results.** Ellipsometry measurements showed that the P(MEO$_2$MA-*co*-OEGMA) copolymer

(28) Harroun, T. A.; Fritzsche, H.; Watson, M. J.; Yager, K. G.; Tanchak, O. M.; Barrett, C. J.; Katsaras, J. *Rev. Sci. Instrum.* **2005**, *76*(6), 065101−1−065101−5.
(29) Kent, M. S.; Majewski, J.; Smith, G. S.; Lee, L. T.; Satija, S. *J. Chem. Phys.* **1998**, *108*(13), 5635−5645.
(30) Sirard, S. M.; Gupta, R. R.; Russell, T. P.; Watkins, J. J.; Green, P. F.; Johnston, K. P. *Macromolecules* **2003**, *36*(9), 3365−3373.
(31) Feng, W.; Zhu, S. P.; Ishihara, K.; Brash, J. L. *Langmuir* **2005**, *21*(13), 5980−5987.
(32) Archambault, J. G.; Brash, J. L. *Colloid Surf., B* **2004**, *33*(2), 111−120.

layers on sample 1 (S1, 5% OEGMA) and sample 2 (S2, 15% OEGMA) were 1228 Å and 1161 Å, respectively. Besides similar thicknesses, both samples had a surface water contact angle of ~40°, indicative of hydrophilic surfaces.

In this work, $Cu^{II}Cl_2$, instead of free initiator, was added to the polymerization solution for good control of ATRP and high graft polymer molecular weight. There were no free polymer chains formed in the solution. As a result, chain length and grafting density of the grafted polymer on the surface could not be estimated. In order to have an approximation, we adopted the grafting density data from our previous work. In the work, homoPOEGMA brushes were grafted from silicon wafer with the same surface-initiated ATRP method.[33] The only difference was the ~4.5 side chain EO units. The grafting density was 0.26 chains/nm$^2$ and the polydispersity was around 1.3, measured from the free polymer in solution. It was assumed that the grafting densities of the copolymer brushes in this work were close to that of homoPOEGMA. The chain length could then be estimated from the equation of $\Gamma = d\rho/M_n$ where $\Gamma$ is the grafting density, $d$ is the layer thickness, $\rho$ is the polymer bulk density, and $M_n$ is the molecular weight. The monomer molecular weights of S1 and S2 are 202.6 and 231.2 g/mol, respectively. A bulk polymer density of 1.0 g/cm$^3$ was assumed. The estimated chain lengths of the S1 and S2 polymers were 1400 and 1150 OEGMA monomeric units, respectively. It should be noted that these chain lengths could be overestimated because the copolymer side chain length of ~2.5 EO units is smaller than 4.5 of homoPOEGMA. The shorter side chains might yield a grafting density higher than 0.26 chains/nm$^2$; therefore, the real chain length could be shorter than the estimated value.

**NR Measurements of Dry Samples.** Samples were first measured in air in order to obtain the dry thickness of the grafts and the parameters needed to subsequently model the hydrated samples. Figure 1 shows the NR profiles for S1 and S2 in air. The three-layer model representing $SiO_2$, the initiator layer, and the polymer brushes was used to fit the data. The theoretical SLDs of Si, $SiO_2$, and air were chosen and kept constant throughout the modeling procedure. Other parameters, including the thickness and SLDs of the initiator and polymer layers were allowed to vary until $\chi^2$ was minimized. The best fits (lines) to the data are shown in Figure 1, with the various model parameters summarized in Table 1. The thicknesses of the S1 and S2 surface polymer layers are 1185 and 1131 Å, respectively. These values are in good agreement with those obtained by ellipsometry.

**Thermoresponsive Behavior of Samples in Water.** Polymer brush conformations of S1 in $D_2O$ were measured at different temperatures. The NR profiles and their best fits are shown in Figure 2a. The data were fitted using the three-layer model (i.e., $SiO_2$, initiator, and polymer layer) along with a stretched parabolic decay (mentioned previously). The initiator/polymer layer SLDs and $SiO_2$ layer thickness were adopted from the dry-state measurements and were fixed during fitting. The validity of the stretched parabolic decay for POEGMA brushes hydrated in water has been previously demonstrated.[34] Using this model, the NR data were well fit, as shown in Figure 2a. In the case of some NR data, the Kiessig fringes were absent as a result of a diffuse polymer/water interface.

The SLD profiles of polymer brushes on the surface were determined from the best fits to the data. They were then easily converted to polymer volume fraction profiles by assuming that
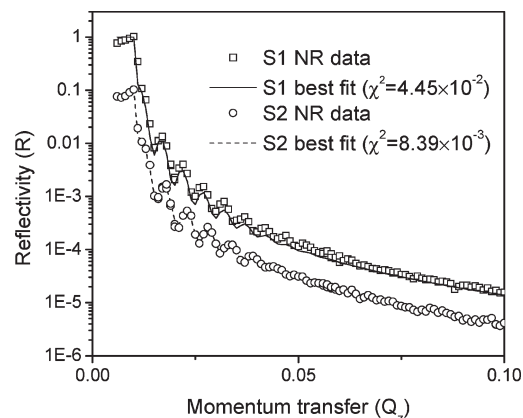
(33) Feng, W.; Chen, R. X.; Brash, J. L.; Zhu, S. P. *Macromol. Rapid Commun.* **2005**, *26*(17), 1383–1388.
(34) Feng, W.; Nieh, M. P.; Zhu, S.; Harroun, T. A.; Katsaras, J.; Brash, J. L. *Biointerphases* **2007**, *2*(1), 34–43.
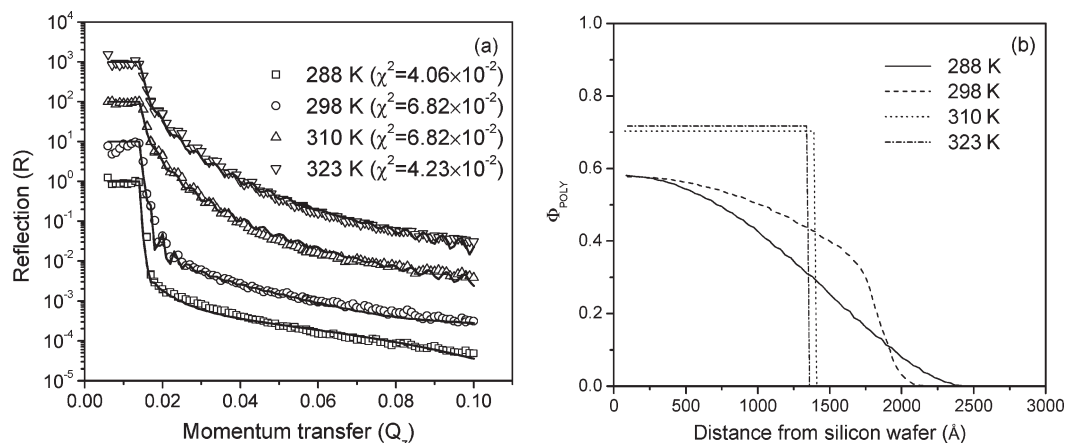
**Figure 1.** Neutron reflectivity profiles for dry samples and the best fits to the data. The curves were offset by arbitrary factors in order to better distinguish the data.

**Table 1. Model Parameters for Surface Grafts in the Dry State**

| species | | SLD ($10^{-6}$ Å$^{-2}$) | thickness (Å) measured from NR | thickness (Å) measured from ellipsometry |
|---|---|---|---|---|
| air | | 0.00[a] | N/A | N/A |
| $D_2O$ | | 6.34[a] | N/A | N/A |
| Si wafer | | 2.07[a] | N/A | N/A |
| $SiO_2$ layer | S1 | 3.48[a] | 16[b] | 14[b] |
| | S2 | 3.48[a] | 16[b] | 14[b] |
| initiator layer | S1 | 0.22[a] | 24[b] | 19[b] |
| | S2 | 0.22[a] | 22[b] | 19[b] |
| polymer layer | S1 | 0.81[b] | 1185[b] | 1228[b] |
| | S2 | 0.73[b] | 1131[b] | 1161[b] |

[a] Theoretical value. [b] Measured value.

the volumes were additive. The SLD for the binary polymer/solvent system can be written as follows: $\rho_{mix}(z) = \Phi_{poly}(z) \times \rho_{poly} + [1 - \Phi_{poly}(z)] \times \rho_{solvent}$, where $\rho_{mix}(z)$ is the SLD of the polymer/solvent mixture at a distance $z$ from the interface, $\Phi_{poly}(z)$ is the polymer fraction at a distance $z$, and $\rho_{poly}$ and $\rho_{solvent}$ are the SLDs of the polymer and the solvent, respectively.

The polymer volume fraction profiles of S1 at four different temperatures are shown in Figure 2b. At 288 K, the polymer brushes were well extended into water. The swelling ratio, defined as the thickness of the polymer layer in water divided by the thickness of the polymer layer in dry state, was studied. In this work, the thickness of the polymer layer in water was approximated at the distance where the polymer fraction decreased to about 10%. At 288 K, the swelling ratio of polymer brushes in $D_2O$ was approximately 1.8. As EO groups can form hydrogen bond with water, a hydration layer was built up surrounding the polymer chains. As a result, the polymer chains extended completely into water. The fraction of water inside the polymer layer was determined to be greater than 50%, implying that water is a good solvent for P(MEO$_2$MA-*co*-OEGMA) copolymer brushes at low temperatures.

When the temperature was increased to 298 K, there was a slight decrease in the polymer brushes thickness, indicative of a decrease in the affinity between EO groups and water molecules. Although this resulted in a decreased water fraction inside the polymer layer, the average volume fraction of water was still greater than 50%, indicating that P(MEO$_2$MA-*co*-OEGMA) copolymer brushes are still hydrophilic at this temperature.

When the temperature was increased to 310 K (above the polymer's LCST), the polymer brushes collapsed, excluding

**Figure 2.** (a) Neutron reflectivity profiles of S1 in $D_2O$ and the best fits to the data. The curves were offset by arbitrary factors in order to better distinguish the data. (b) Volume fraction profiles of polymer brushes.
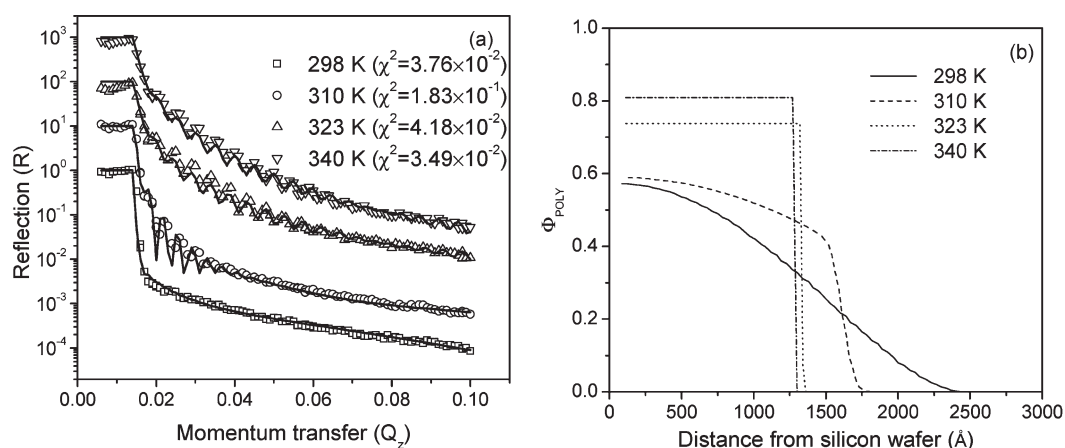


**Figure 3.** (a) Neutron reflectivity profiles of S2 in $D_2O$ and the best fits to the data. The curves were offset by arbitrary factors in order to better distinguish the data. (b) Volume fraction profiles of polymer brushes.

much of the water from the polymer layer. This resulted in the appearance of a distinct interface between the polymer layer and water. The swelling ratio decreased to around 1.2, while the volume fraction of water inside the polymer layer decreased to approximately 30%. When the temperature was increased to 323 K, the polymer layer experienced a further collapse, expelling even more water.

Figure 3a shows NR reflectivity data for S2 and the best fits to the data (solid lines) at four different temperatures. The polymer volume fraction profiles are shown in Figure 3b. For S2, the composition of OEGMA with 9 EO repeat units was increased from 5% (S1) to 15%. As a result, its LCST in water was determined to be around 321 K, higher than that of S1 (305 K). As shown in Figure 3b, at 298 K the polymer brushes extended into $D_2O$, indicating a well-developed hydration layer around the polymer chains. The swelling ratio was approximately 1.8, similar to that of S1 at 288 K.

When the temperature was increased to 310 K, the polymer brushes were obviously compressed and the swelling ratio decreased to around 1.4. An interface formed between the water and the polymer layer, which indicated that the hydration layer surrounding the polymer chains was partially destroyed at a temperature close to the polymer's LCST. Despite the fact that at this temperature the polymer chains were not as extended as those at low temperature, the volume fraction of water inside the polymer layer was still greater than 50%, much higher than the

amount of water in collapsed polymers. At this temperature, the polymer chains were still not in the collapsed state yet.

When the temperature was raised to 323 K, higher than the polymer's LCST, the polymer brushes collapsed. The swelling ratio was determined to be less than 1.2, while the water volume fraction inside the polymer layer was around 30%. When the temperature was 340 K, the polymer layer swelling ratio was only around 1.1, while the water fraction further decreased to about 20%.

**Effect of Salts.** For the application in biomedical devices, the effect of salts must be taken into consideration. Salts are well-known to change polymer solubility in water by disrupting the hydration structure surrounding the polymer's chains. This so-called "salting out" effect may change LCST of the thermoresponsive polymers.[35,36] As a result, the presence of salts affects performance of the thermoresponsive behavior. On the other hand, in some cases, this effect was employed to design "salt-responsive" polymers.[37]
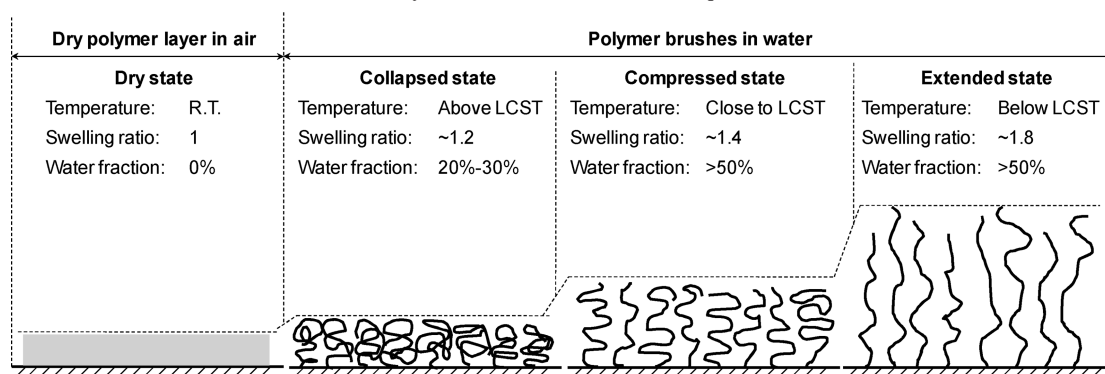
Polymer brush conformations in TBS buffer were measured and compared to those in pure $D_2O$. The results showed that salt

(35) Van Durme, K.; Rahier, H.; Van Mele, B. *Macromolecules* **2005**, *38*(24), 10155–10163.
(36) Zhang, Y. J.; Furyk, S.; Bergbreiter, D. E.; Cremer, P. S. *J. Am. Chem. Soc.* **2005**, *127*(41), 14505–14510.
(37) Magnusson, J. P.; Khan, A.; Pasparakis, G.; Saeed, A. O.; Wang, W. X.; Alexander, C. *J. Am. Chem. Soc.* **2008**, *130*(33), 10852–10853.

**Scheme 2. Polymer Brush Conformation in Aqueous Solutions**

differentially affected polymer brushes, depending on their conformational state. In order to clarify the salt effect, polymer brush conformations are subdivided into three states (i.e., extended, compressed, and collapsed states), as shown in Scheme 2.

When the hydration layer around the polymer chains is well developed, the chains extend deeply into the bulk water, exhibiting a swelling ratio of approximately 1.8 and a water volume fraction of greater than 50%. The polymer brushes in this state are defined as being extended (S1 at 288 K and 298 K, S2 at 298 K). When the temperature is close to the polymer's LCST, hydrogen bonds between the EO groups and water molecules are significantly affected, with the hydration layer undergoing partial degradation. In this case, the polymer chains are not well-extended in water. Although water volume inside the polymer layer is still greater than 50%, the swelling ratio decreases to around 1.4. An interface between the polymer layer and water is formed, and the polymer brushes are described as being in the compressed state (S2 at 310 K). When the temperature is above the polymer's LCST, polymer brushes collapse and the swelling ratio decreases to approximately 1.2. The water faction of the collapsed polymer is about 30%.

The thermoresponsive P(MEO$_2$MA-*co*-OEGMA) in solution undergoes a sharp phase transition as PNIPAM does.[12] Huck et al.[16] also observed a sharp collapse transition in their experiment. The collapse occurred within a 10 °C temperature range. In the present work, three states were observed. However, only the transition from the compressed state to the collapsed state is considered to be a phase transition and it is very sharp considering that the temperature range was smaller than 10 °C. The transition of from the extended state to the compressed state was gradual caused by the change in swelling ratio. Both of the states had water fraction larger than 50%. There was no phase transition happened in this range.

When the polymer brushes are in the extended state, there is a well-developed hydration layer around the polymer chains. The presence of salt had the greatest impact on the extended polymer chains because of its significant disruption of the hydration layer. As shown in Figure 4, in TBS buffer the polymer chains on S1 at 298 K were more compressed than in pure water. Distinct changes in the swelling ratio were also observed. Chain conformation changed from the extended state, in pure water, to the compressed state in TBS buffer because of the partial disruption of the hydration layer by the salt.

For the polymer brushes in the compressed region, for example, S2 at 310 K, the effect of salt was less pronounced. As shown in Figure 4, the polymer chains in TBS buffer compressed only slightly. The reason was that the hydration structure around the polymer brushes in the compressed state was already partially
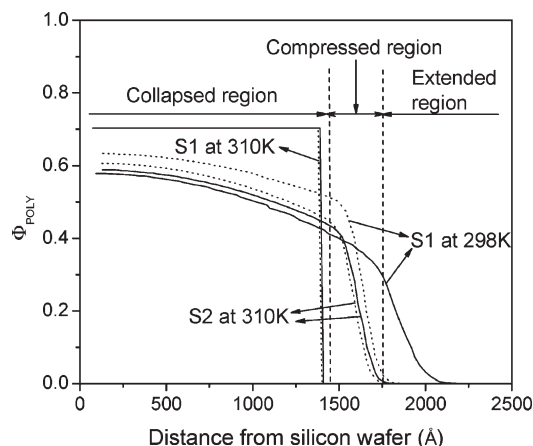


**Figure 4.** Volume fraction profiles of polymer brushes. Solid line: in pure D$_2$O. Dotted line: in TBS buffer.
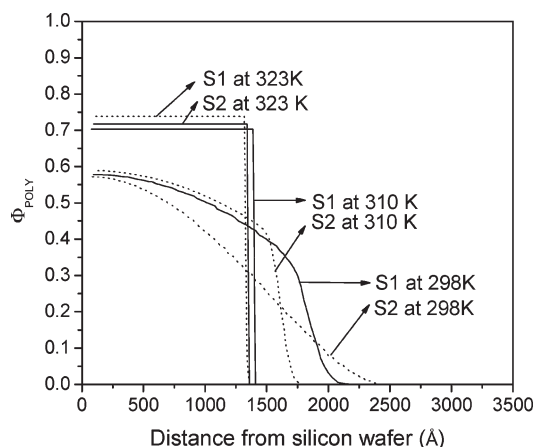


**Figure 5.** Volume fraction profiles of S1 and S2 polymer brushes.

destroyed because of the elevated temperature. As a result, when salt was added, the "salting-out" effect did not have significant impact on the polymer conformation, as it had on well-extended polymer chains. For collapsed polymers (e.g., S1 at 310 K), the presence of salt had no effect on the polymer conformation, as the affinity between polymer segments was greater than that between EO groups and water.

**Effect of Copolymer Composition.** In Figure 5, the conformations of polymer brushes on S1 and S2 are compared at three different temperatures in order to elucidate the effect of copolymer composition on their thermoresponsive behavior.
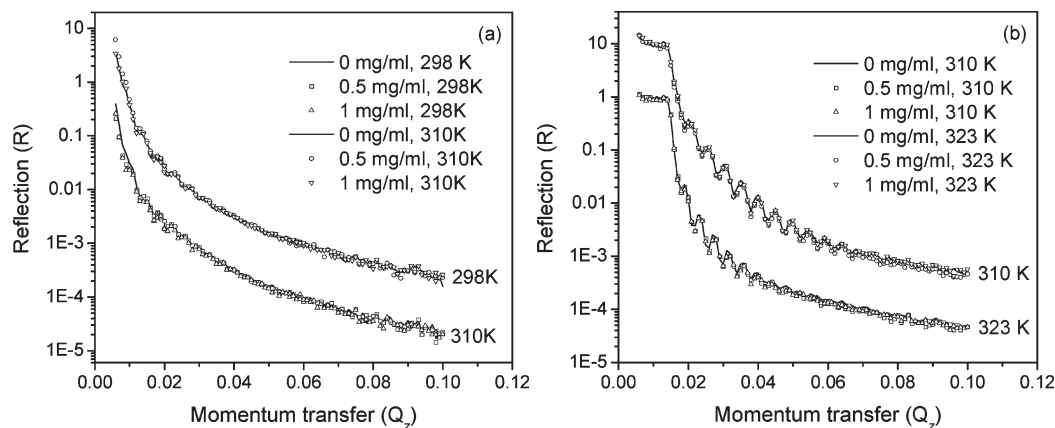
**Figure 6.** Neutron reflectivity profiles of (a) S1 and (b) S2 in TBS buffers with lysozyme. The curves were offset by arbitrary factors in order to better distinguish the data.

At room temperature (298 K), both two composition designs gave extended polymer brushes on the surface. However, the higher OEGMA composition brushes (i.e., S2 with 15% OEGMA) had a better affinity for water, which enabled the copolymer chains to extend more deeply into the water.

At around 310 K, the polymer brushes with 5% OEGMA on S1 were already in the collapsed state, while those with 15% OEGMA on S2 were still extended. However, because the temperature was close to the S2 sample's LCST, the affinity between EO groups and water became less favorable, the polymer brushes were in the compressed state. At 323 K, both S1 and S2 brushes were in the collapsed state, with no significant difference in the polymer brush conformation. Moreover, they exhibited the same swelling ratio (~1.2) and water volume fraction within the polymer layer.

**Effect of Protein.** Besides salt, various proteins inside the human body may also affect the conformation of polymer brushes. Here, we studied the possible impact of lysozyme on polymer brush conformation. Lysozyme is abundant in some secretions, e.g., tears, saliva, mucus, and so forth. The lysozyme used in this work is from chicken egg white. The conformations of S1 and S2 in TBS buffer at two different protein concentrations (i.e., 0.5 mg/mL and 1 mg/mL, respectively) were investigated. The measurements were performed at two different temperatures, one below the polymer's LCST, and the other above. As shown in Figure 6, at the same temperature, the NR curves with different protein concentrations overlapped. This showed that the addition of lysozyme had no effect on polymer brushes conformation, regardless of their conformational state.

**Protein Adsorption Resistance.** As shown in Figure 7, the bare silicon wafer adsorbed around 800 ng/cm$^2$ of lysozyme at room temperature. In comparison, the amount of lysozyme adsorbed on S1 and S2 surfaces at room temperature was around 40 ng/cm$^2$, which meant a 95% reduction in protein adsorption. Surfaces grafted with homoPOEGMA (with 4.5 repeat EO units) brushes were also studied as comparison. As can be seen, the protein adsorption resistance performance of S1 and S2 modified with the current copolymer brushes was close to the surface grafted with homoPOEGMA containing 4.5 repeat EO units.

In most cases, an increase in temperature results in increased protein adsorption. For the present studies, when temperature was increased to 323 K the adsorbed protein amount on bare silicon increased to around 1150 ng/cm$^2$. At 323 K, the polymer brushes on S1 and S2 were both in the collapsed state; however, the amounts of adsorbed protein were still very low, close to those
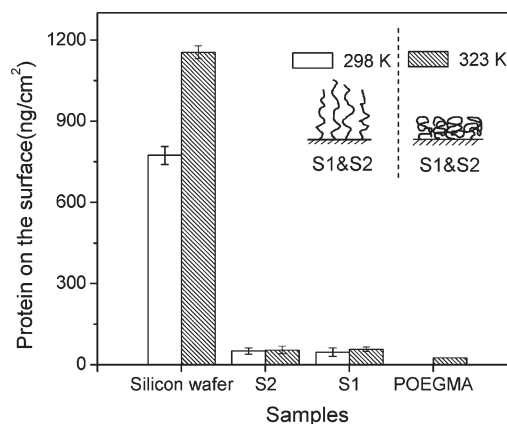


**Figure 7.** Lysozyme adsorption on the surfaces at different temperatures.

at room temperature. This finding of no significant difference between the extended and collapsed states in protein repelling performance is somewhat interesting. It is well-known that protein adsorption is affected by various interactions between components in the system (e.g., protein, water, surface, and other solutes). The change to the overall Gibbs energy determines the final equilibrium state: $\Delta G = \Delta H - T\Delta S$, where $H$, $S$, and $T$ are enthalpy, entropy, and temperature, respectively. In the case of protein adsorption, the change to the Gibbs energy must be negative. In different systems, protein adsorption can be either entropically or enthalpically driven.

The enthalpy is believed to be the main factor for the surfaces grafted with PEO to resist protein adsorption. The change in enthalpy is associated with several factors during the protein adsorption process: e.g., van der Waals, electrostatic force, hydration forces, and hydrophobic interactions. The highly repulsive hydration force from the surfaces with tethered PEO is the main force in repelling proteins. Here, the polymer layers remain hydrophilic in both the extended and collapsed states, thus effectively reducing protein adsorption. As mentioned, at temperatures below the LCST, the polymer chains extended deeply into water with a well-developed hydration layer surrounding the polymer chains. However, at temperatures above the polymer's LCST, the affinity between polymer segments is larger than that between EO groups and water, causing the polymer brushes to collapse. Nevertheless, the water fraction inside the collapsed polymer layer is still greater than 20% (Figure 2b and Figure 3b], i.e., the polymers remain hydrophilic.

As a result, at the polymer−water interface a hydration layer is probably still present, effectively resisting the adsorption of protein.

## Conclusions

In conclusion, PEG-based thermoresponsive surfaces were prepared by grafting P(MEO$_2$MA-*co*-OEGMA) copolymer brushes on silicon wafers via the surface-initiated ATRP method. The detailed conformation information of the polymer brushes in aqueous solutions as a function of temperature was obtained using the NR method. Polymer conformation changed from the well-extended state to the compressed state, and subsequently to the collapsed state with increased temperature. The addition of salt was found to affect the brushes differentially, depending on the development of the hydration layer around the polymer chains. For well-extended polymer brushes in water, salt strongly influenced the polymers conformation, most likely by significantly disrupting the hydration layer surrounding the brushes. On the other hand, in the case of compressed and collapsed polymer brushes, the addition of salt had little effect. The presence of protein (lysozyme) in solution did not impact polymer conformation. The current thermoresponsive surfaces were found to have good protein adsorption resistance. Both extended and collapsed copolymer brushes gave good protein repelling performance.